



Hartley, J., & Ward, C. (2017). Improving the Understanding of Tufted Energy Absorbing Sandwich Structures. In *Proceedings of the thirty-second technical conference* (pp. 2260-2273). American Society for Composites. <https://doi.org/10.12783/asc2017/15347>

Peer reviewed version

Link to published version (if available):
[10.12783/asc2017/15347](https://doi.org/10.12783/asc2017/15347)

[Link to publication record in Explore Bristol Research](#)
PDF-document

This is the author accepted manuscript (AAM). The final published version (version of record) is available online via American Society for Composites at <https://cdmhub.org/groups/asc2017/program>. Please refer to any applicable terms of use of the publisher.

University of Bristol - Explore Bristol Research

General rights

This document is made available in accordance with publisher policies. Please cite only the published version using the reference above. Full terms of use are available:
<http://www.bristol.ac.uk/red/research-policy/pure/user-guides/ebr-terms/>

Improving the Understanding of Tufted Energy Absorbing Sandwich Structures

JAMIE HARTLEY, and CARWYN WARD

ABSTRACT

Tufting has been shown to be an effective method for improving the performance of sandwich structures against edgewise impact loading. However, the mechanisms that take place during failure, and the role the tufts play within this are not well characterised. Experimental testing has therefore been carried out to improve the understanding of the failure behaviour of these structures, with the particular focus of this study being on investigating the behaviour of the tufts themselves. Firstly quasi-static edgewise crushing tests were carried out to visually identify the failure behaviour of the tufts, indicating that the tufts ‘drift’ and collide as they fail. Follow up testing was then carried out on the interaction between the tufts and the surrounding foam core. Whilst it was observed that single tufts only have a very small contribution to the overall energy absorption of a tufted panel, this contribution can increase significantly with the addition of multiple tufts, and allowing interactions to occur between them. This behaviour could therefore be designed into the structure to help maximise the energy absorption during an impact event.

INTRODUCTION

Due to the increasing legislative pressure on Automotive manufacturers to reduce emissions and increase fuel efficiency [1], there is a shift within the industry towards the use of lightweight fibre-reinforced polymer (FRP) composite structures [2]. In particular, composite sandwich structures are seen as an effective way of increasing structural stiffness whilst maintaining low weight, and have the added potential of vibration damping and noise insulation [3], a key requirement for use in automotive vehicles.

For any material or structure to be considered for an automotive application, it must be capable of protecting the occupants from the large forces experienced during a crash. One of the most difficult cases to design for is an edgewise impact from a

narrow roadside object such as a lamppost or utility pole, as there is little room to dissipate the energy of the concentrated impact. Whilst the use of FRPs is potentially a lightweight design solution due to the brittle failure of the material potentially absorbing more energy than current metallic structures [4], the use of FRPs within safety systems is currently limited to the high performance and motorsport sectors. For sandwich structures in particular, an inherent weakness at the interface between skin and core can lead to a catastrophic unstable collapse of the structure, under an edgewise impact load, which is not an efficient, or safe energy absorbing mechanism [5].

Amongst other through-thickness reinforcement methods [6,7], tufting has recently stood out as a technique for reinforcing the weak interface of a sandwich structure, and improving the failure behaviour, by mechanically tying the skins and core together. Tufting originated as an ancient carpet manufacturing technology but has recently gained popularity as a method of through-thickness reinforcement for composite materials. Unlike more traditional stitching methods, tufting uses a single threaded needle to insert a reinforcing thread, and relies on friction alone to hold the reinforcement in place [8]. As only a single needle is used, the surface features of the reinforcement are not symmetric, with a seam of thread formed on the insertion side, and a loop of thread formed on the back face. The advantages of tufting over more conventional methods stem from the need for only one needle. A single needle means access is only needed to one side of the preform, increasing the allowable manufacturing complexity. There is also less damage to the preform from the use of multiple needle insertions [9]. Finally, the use of friction to hold the reinforcement in place means that reduced crimping of the fabric takes place, compared to traditional stitching methods, which better maintains the in-plane mechanical properties of the final cured part [10,11]. However, use of the technology is still limited, with understanding of the influence of the manufacturing process on performance [9], as well as the development of suitable design tools [12] still at an early stage.

Over the past decade, several researchers have explored and demonstrated the advantages of tufting in both monolithic and sandwich structures under a range of design cases [13–16]. More recently, a study of particular interest by Blok et al. [17] demonstrated the potential of tufts to improve the crashworthiness of sandwich structures under edgewise loading. They found that the use of tufts restrained the separation of skin and core, resulting in increased fracturing within the facesheets, which led to a greater amount of energy absorbed. Whilst these performance improvements are a positive step forward for the technology, a better understanding of the failure mechanism is required to be able to make informed design choices in the future. An investigation by Hartley et al. [18] explored the ‘unit cell’ of a tufted panel, focusing on the effect of manufacturing process variables such as the tuft length and local density on mechanical performance. Whilst it was seen that tuft length had very little effect on performance it was found that the tuft thickness and local density, did.

A key observation made from this work was the presence of columns of resin around the tufting threads within the foam core (Figure 1). These are formed due to the process of inserting the tufting needle into the preform leaving a complimentary void within the foam core. During subsequent resin infusion, these voids fill with resin, which on curing leaves an array of rigid columns within the core. Analysis of failed test samples has indicated that these columns reposition during the crushing mechanism, suggesting they play a role in the energy absorption of the structure.

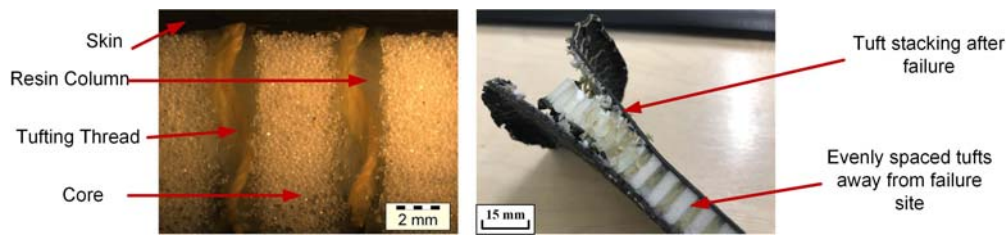


Figure 1. Resin column morphology, formed as a result of the tufting process.

An understanding of how this mechanism takes place, and the influence it has on performance could allow for it to be incorporated into the design of future sandwich panels, and thus help improve their structural efficiency. This paper will outline novel test methods used to capture this behaviour, and then to quantitatively evaluate its contribution to the overall performance of the structure.

METHODOLOGY

Experimental testing was carried out in two stages. Firstly, tufted sandwich coupons were tested in edgewise compression to observe and capture the failure behaviour. Follow up testing was then carried out to look specifically at the interaction of a resin column within the foam core.

Edgewise Compression Testing

SPECIMEN MANUFACTURE

Two sandwich panels (600 mm x 500 mm) were manufactured for testing using the Vacuum-Assisted Resin Transfer Moulding (VARTM) process. The skins were formed using a unidirectional non-crimp fabric by SGL Automotive (300 gsm), with a stacking sequence of $[0/90/0]_s$, and the total thickness of each skin was approximately 2 mm. The core was a 10 mm thick Rohacell® 110 IG-F closed-cell foam from Evonik, giving a total cured panel thickness of 14 mm.

Tufting of one of the panels was carried out using a KUKA robot and KSL tufting head, based at the National Composites Centre (Bristol, UK). The preform was stabilised by heating for 2 hours at 90°C under vacuum pressure to activate the binder in the carbon fabric. A Tkt-20 Kevlar® thread (from Somac Threads UK) was used for the TTR, with a tuft spacing of 6 mm by 6 mm, chosen in order to match previous works in the testing of tufted sandwich structures [17,18]. The other panel was left untufted, to act as a benchmark for testing. The preform was then infused using the Vacuum-assisted resin transfer moulding (VARTM) process at 40°C using EPIKOTE® Resin RIM 935 and EPIKURE® Curing Agent RIM 936 by Momentive. The cure cycle was two hours at 60°C, followed by a two-hour post-cure at 90°C.

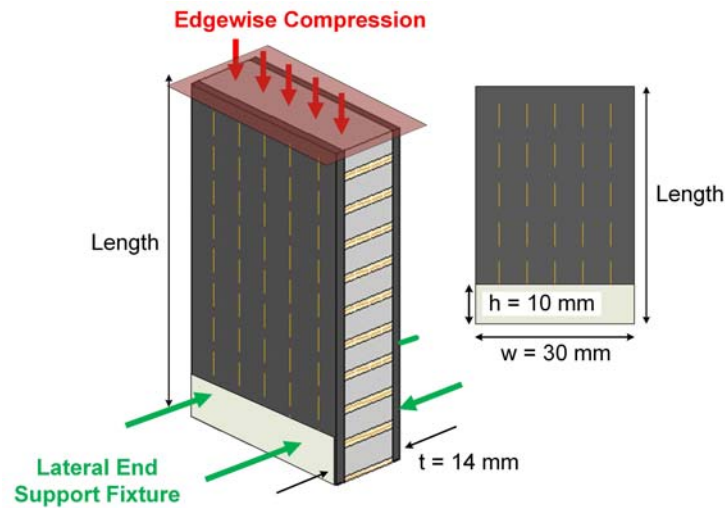


Figure 2. Configuration and dimensions of the sandwich test coupons.

Table I. Test Coupon Properties

Group	Length (mm)	CV (%)	Average Mass (g)	CV (%)
Reference	50	0.14	13	3.1
A	40	0.18	12	3.4
B	50	0.03	16	2.6
C	60	0.17	19	2.1

The two panels were cut into test coupons using a diamond blade, taking care to ensure that for the tufted panel a line of tufts was located, and thus visible, along one edge of the coupon. Polishing of the tufted edge was carried out to improve the clarity of the resin and thus aid tracking of the tufts. This was achieved using a Buehler MetaServ 250 Grinder-Polisher with P400 SiC abrasive paper at 350rpm and a constant water flow to clear excess particles and avoid scratching the coupon surface. The coupons were then allowed to dry naturally at room temperature for a period of several hours. The coupon geometry was rectangular as shown in Figure 2, with the coupon length chosen as a test variable as shown in Table I. The mass of the coupons was recorded to allow for normalisation of the energy absorbed, and the dimensions of each coupon were also measured using a digital Vernier calliper to check for accuracy and consistency.

TEST PROCEDURE

Testing was carried out under quasi-static loading conditions using a Zwick 1466 test machine. To ensure failure occurred at the free end, the coupons were clamped at the base within an end support fixture, and positioned at the centre of the loading plates, as shown in Figure 3. Coupons were aligned such that the long edge was parallel to the crushing direction, with the polished face exposed for tracking. The loop face of the coupon was also kept on the right hand side for each test.

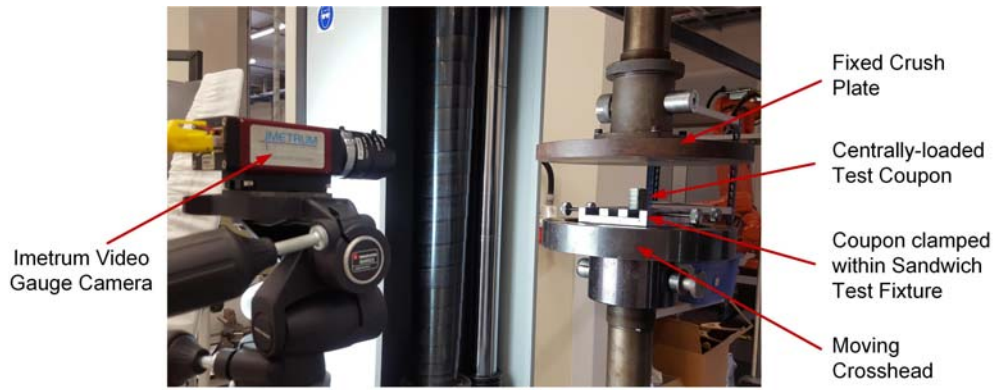


Figure 3. Edgewise compression testing setup.

A displacement control program was used to provide a constant quasi-static crushing rate of 2 mm/min. Testing was terminated after crushing of the coupon had reached the final tuft before the fixture. A total of 3 coupons were tested per configuration. An Imetrum[®] video gauge system was used to track the movement of the tuft columns at the edge of the coupon. This camera system was able to track the movement of individual pixels within an image, thus following the movement of the tufts as the coupon was crushed. White paint marks were placed on each tuft to act as clear tracking points. The system also allowed video playback of test, allowing failure mechanisms to be viewed and identified.

Load-displacement data was tracked and output by the test machine for analysis. A key metric in automotive design for determining the capability of composite materials as energy absorbing devices is the Specific Energy Absorption (SEA) [19]. The SEA can be derived as Equation 1:

$$SEA = \frac{W}{\rho A \delta} = \frac{\int_0^{\delta} F dx}{\rho A \delta} \quad (1)$$

Where W is the work done on the structure during crushing (force x displacement), and $\rho A \delta$ defines the mass of the crushed material. The SEA was approximated by integrating the area under the load-displacement curve using the midpoint rule and then dividing by the crushed mass of the coupon. To approximate the mass of the crushed material, an average areal sandwich density was found by using the surface area of the test coupons shown in Figure 2 and dividing by the coupon mass. By calculating the surface area of the coupon over the chosen crushing distance, the material density could then be used to find the crushed material mass. Whilst the mass distribution through the coupon is not homogeneous as a result of the discrete tufts, the relatively high density of tufts should ensure consistency between coupons and thus an acceptable level of error.

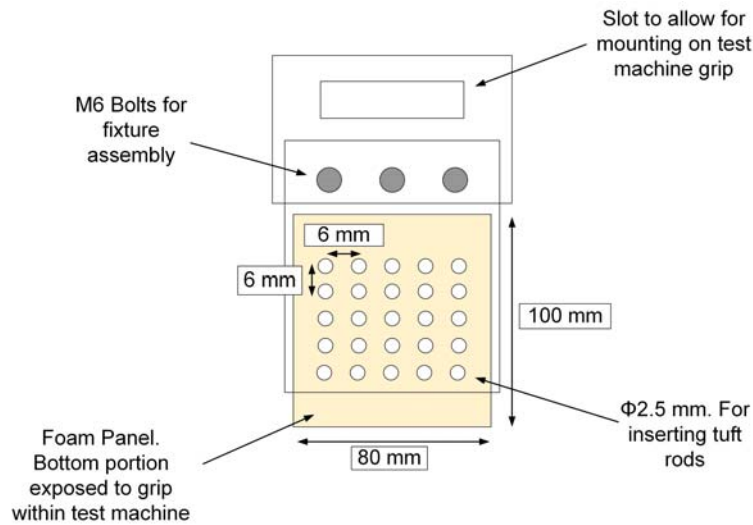


Figure 4. Column ‘drift’ test fixture design

Column-Core Interaction Testing

TEST PROCEDURE

To simulate the behaviour of the tufts during failure, a novel test fixture was developed, capable of pulling arrays of replica columns through a foam panel. Pulling of the columns was required as a compressive method would have led to buckling due to the instability of the foam when unsupported by the facesheets. The design of the fixture allowed for the insertion of multiple pins, to simulate different tufting configurations. The spacing between each hole was 6 mm, to match the minimum spacing used in previous testing [17]. The fixture was laser cut from transparent Perspex sheets of 10 mm thick, to allow visual tracking of the pins as they moved through the foam. The design of the test fixture is shown in Figure 4.

Load was applied to the specimen using a Shimadzu desktop electromechanical test machine, with a 1kN load cell. The upper part of the fixture featured a slot for the upper stage grip of the test machine to slot into, whilst at the bottom a section of the foam was left exposed and was mounted in the lower test grip, as shown in Figure 5. Sand paper (P60 grit) was used to increase the friction between sample and loading grip, and avoid slipping. The loading rate applied was 4 mm/min. An Imetrum[®] video gauge system was used for visual tracking of the test, following the movement of the pins as they moved through the foam. The system also allowed video playback of the test, allowing failure behaviour to be viewed and identified.

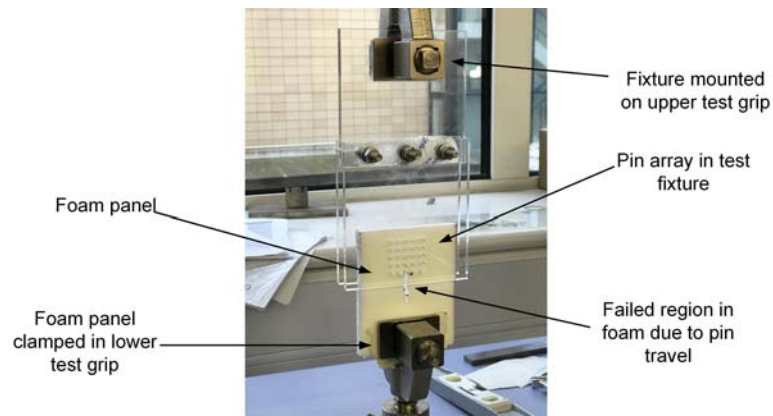


Figure 5. Setup of test fixture on Shimadzu test machine.



Figure 6. A comparison of a tufted resin column (left) and the steel pin used (right).

SPECIMEN MANUFACTURE

For the materials selection, Rohacell® 110 IG-F foam was again used for the core. To simplify the test setup, rigid steel pins of 2.3 mm diameter (equivalent to the largest diameter of the tufting needle) were chosen to simulate the tufts (Figure 6). This choice was also made to avoid any deformation or fracture of the simulated columns taking place during testing. As can be seen from the image, the use of a steel pin can be seen as an idealised case, as the surface roughness of the foam and the subsequent resin infiltration leaves a very rough and uneven surface on the resin column. Due to the needle insertion, fragments of foam may also break off around the hole leaving a slightly larger diameter resin column than would be expected from the dimensions of the needle. Whilst differences do exist, the smooth surface and slightly narrower diameter of the steel pin will allow for conservative estimates of the energy absorption of the process to be made.

To insert the pins, a small pin hammer was used to gently tap them into the foam panels. This was done to ensure a tight fit between the pin and the surrounding foam. The steel pins were cut slightly longer than the through thickness dimension of the foam and test fixture, in order to allow load to be applied to the pin as the test fixture began to move. To simulate collisions between tufts additional pins were used, but were cut

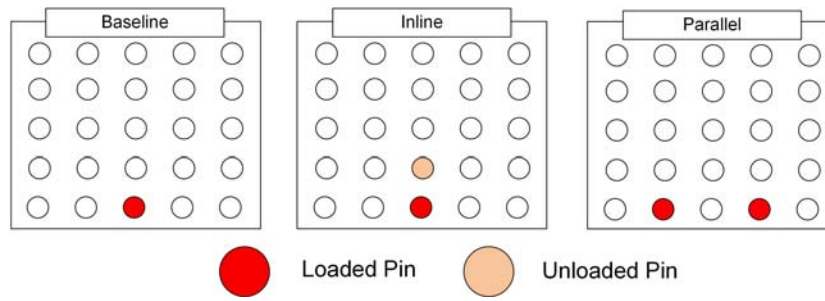


Figure 7. Positioning of loaded and unloaded for each test configuration considered.

slightly shorter than the foam thickness so they would sit between the two inner surfaces of the fixture and thus could move freely through the foam.

A total of three test configurations were used, with varying locations and numbers of rods inserted to simulate different tuft configurations. Initially a baseline set of data was created, using a single, centrally positioned rod. Further configurations were then created to explore the effects of multiple rods, firstly by testing two rods in line with each other to simulate a collision between them, followed by loading two rods in parallel with each other. A summary of the test configurations and their naming conventions is given in Figure 7. Those rods that are loaded and those that are not are highlighted in the figure.

RESULTS AND DISCUSSION

Edgewise Compression Testing

As expected, the failure of the coupons during edgewise compression testing followed previously observed trends [5,17], where the untufted reference coupons failed in an unstable and unpredictable manner, an example of which can be seen in Figure 8, where the untufted coupon has failed by disbonding of the facesheets and collapse of the foam core. In comparison in the same figure, the tufted coupon exhibits a stable progressive splaying failure of the facesheets, as the interface with the core remains intact for a longer period. Representative load-displacement traces for a tufted and untufted coupon are shown in Figure 9, and these follow a common trend of a peak load followed by a sustained crushing load. There is a clear difference between the relatively high crushing load of the tufted coupon, compared to the unstable failure and reduced load carrying ability of the untufted coupon. A summary of the test results obtained from edgewise compression tests is presented in Table II. The results show a general increase in energy absorption of the tufted coupons compared to the reference coupons. The majority failed in a stable manner but several did not and these are highlighted in grey. None of the reference coupons tested exhibited a stable failure mechanism.

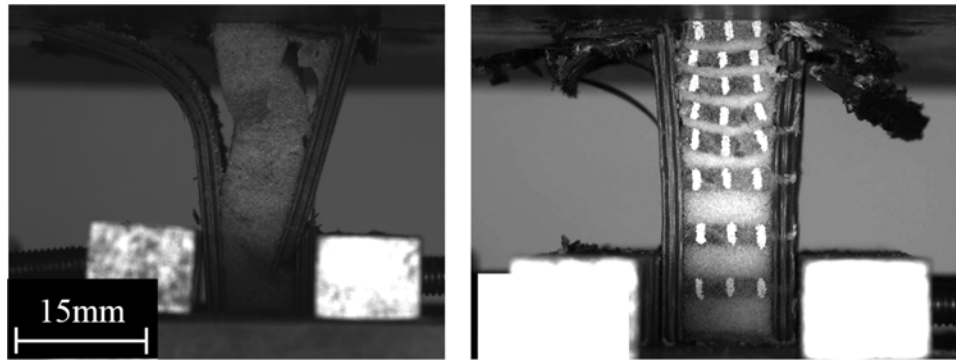


Figure 8. Comparison of failure mechanisms in untufted (left) and tufted (right) sandwich coupons.

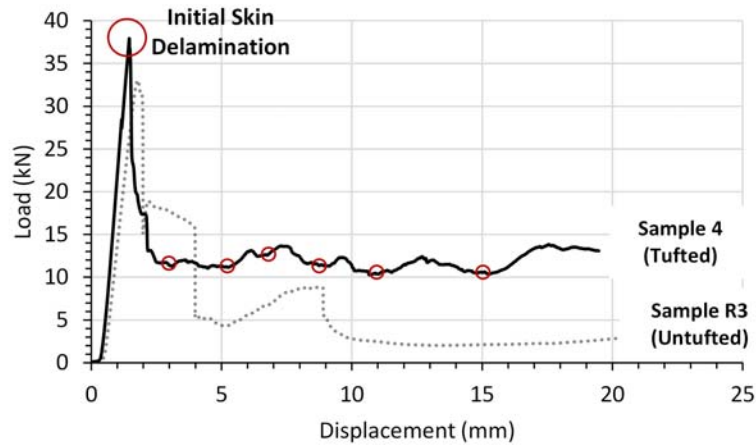


Figure 9. Representative load-displacement curves for a tufted and untufted coupon.

Table II. Summary of Key Test Results of Each Coupon Tested

Group	Crush Distance	Peak Load	Average Crush Load	Average Energy Absorption	SEA
-	<i>mm</i>	<i>kN</i>	<i>kN</i>	<i>kJ</i>	<i>kJ/kg</i>
Reference	13.30	32.82	12.13	0.24	54.42
A	18.54	25.04	14.37	0.30	48.27
B	21.60	32.02	13.33	0.33	43.53
C	28.58	34.60	11.60	0.38	37.73

Following the initial failure within the facesheets, a progressive crushing mechanism began to take place, as shown in a time-lapse image in Figure 10. As the pristine coupon (Figure 10-A) was loaded, initially disbonding occurred between the facesheets and the core, causing them to splay outwards. As the facesheets gave way, the uppermost face of the core became exposed to the crush plate and crushing of the foam began to take place.

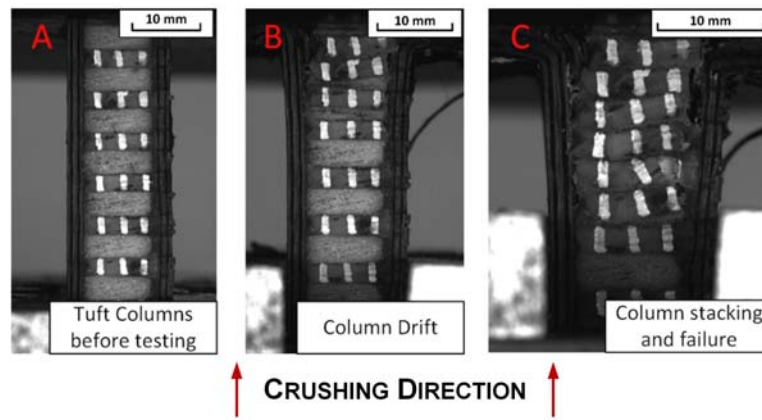


Figure 10. Progressive crushing mechanism observed in tufted sandwich structures. A) Tuft positioning before testing. B) Separation and subsequent ‘drifting’ of tufts. C) Stacking and failure of tuft resin columns.

As the foam was compressed, its density increased significantly until it reached a point where it became rigid. At this stage the uppermost tuft within the coupon, which was in contact with this foam, could no longer move upwards with the motion of the crosshead as it was being held against a rigid surface. The subsequent motion of the rest of the test coupon moving upwards relative to the now fixed tuft created a shear stress at the interface between resin column and facesheet, as well as through the tufting thread. As the upwards motion of the test coupon continued, this crushing behaviour repeated itself, with the gap between the first failed tuft and the next in line closing as the separating foam was crushed. Once the gap between these two tufts was closed they both became locked up against the crush plate and could no longer move (Figure 10-B). This mechanism continued until each of the tufts within the coupon had ‘stacked’ on top of each other and could no longer move. Once this stage had been reached there was almost no foam visible between the tufts, as the foam had been compressed significantly (Figure 10-C).

An example of the tracking results recorded by the video gauge system is shown in Figure 11. Each of the curves within the figure represents the position, relative to the fixed crush plate, of the centre point of each tuft within the coupon. The sequential motion of the tufts discussed previously is clearly indicated in this diagram. As the coupon was loaded the material at the top began to crush and the uppermost tuft started to move. After a short distance this tuft struck the impact plate and could no longer travel any further. This is shown by the flattening of the curve in the figure. Each subsequent tuft then sequentially moved towards the crush plate until they strike the preceding tuft and the curve flattens. The initial gradient of the curves is approximately 2 mm/min which shows that the column movement is strongly dependent on the loading rate of the test machine. This indicates an element of control of the failure mechanism, as it is dependent on the spacing between the tufts. As the movement and location of the tufts during failure is so consistent and predictable, it may be possible to feed this knowledge into the design of the tuft locations. The behaviour of the tufts under a given load case could be designed to ensure that the structure fails in a desired manner, or that failure does not propagate beyond a safe design limit.

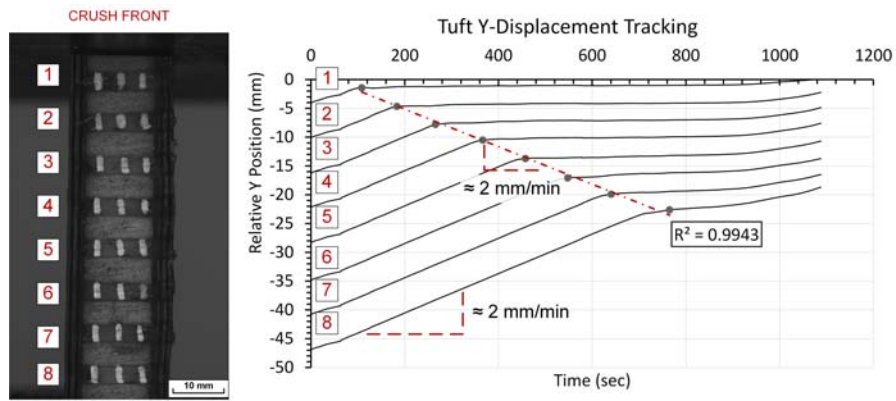


Figure 11. Relative positions of each tuft to the crush plate over time.

The fact that the tufts remain present within the structure will mean that they play a role, even after failure, through frictional effects as well as internal crushing of the foam core. Analysis of the tracking results also revealed the distance that each tuft travelled before stopping. It was found that whilst the spacing between the centre lines of each tuft was defined as 6 mm during panel manufacture, the distance travelled in reality was only around 3 mm. This is due to the relatively large diameter of the resin columns that form during manufacture. The size of the needle used to insert the tufts is approximately 2.5 mm in diameter. This creates a resin column that is much greater in diameter than the tufting thread and thus reduces the 6 mm spacing defined. It was observed that whilst the distance travelled was smaller than predicted, it was consistent across each of the tufts, which indicates a high consistency of the manufacturing process and tuft behaviour.

Column Interaction

The averaged load-displacement traces for the three configurations tested are shown in Figure 12. In each case, the load increased sharply at first, until the foam surrounding the rod began to fail, and the rod started to move. After this point the load increased gradually in each test configuration. Beyond this point the rod begins to slide through the foam sheet (Figure 13-A). As the rod slides, it compresses material in its path, resulting in a gradual increase in load as the test progressed. For the inline test configuration, there is a secondary increase in load at approximately 3 mm of displacement. This is the point at which the loaded and unloaded rods begin to collide with each other, and the unloaded rod is driven through the foam (Figure 13-B). As a result of the rods colliding with each other there is a sustained offset in load compared to the baseline test. However, after approximately 24 mm of displacement, there is a sudden sharp drop in load in the inline curve. This is a result of the loaded rod reorienting its path through the foam, and moving around the unloaded rod ahead of it. It was observed during testing that in a number of cases the loaded rods would slide around the unloaded rods, as seen in Figure 13-C. Similar behaviour has been observed in metallic structures, where compressive residual stress around rods can cause redirection of fatigue cracks [20]. However, it is not clear at this stage if this behaviour is occurring here.

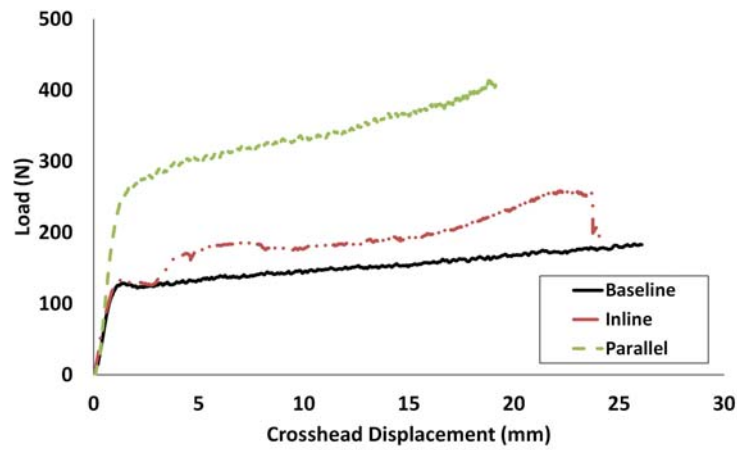


Figure 12. Load-displacement curves obtained from column interaction testing.

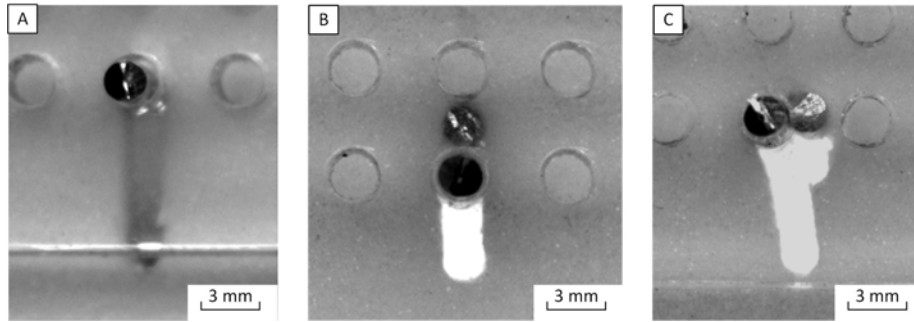


Figure 13. Sliding mechanism of rods through foam. A) Single rod baseline. B) Two rods inline moving together. C) Two rods inline, loaded rod realigning to avoid unloaded rod ahead.

After this event occurs the rod is only pushing against foam again, hence the reduction in load. In the case of the parallel rod tests, the initial loading peak rises above the other two tests. It can be seen from the results that the load is approximately double the baseline as a result of loading two rods in parallel, due to the requirement to crush the foam in two different locations. The gap between the rods was varied during testing, but this had no effect on the load. Another noticeable difference when compared to the baseline was the smooth transition from the initial rapid load increase phase to the rod moving stage. This may be due to the increased number of rods stopping rotation of the sample, and thus eliminating any sudden changes in load.

Energy Absorption

The specific energy absorbed during the tests was calculated for each sample by accounting for the mass of foam crushed in the path of the loaded rods. As can be seen from the results in Table III, the efficiency of energy absorption increased when the rods were allowed to collide with each other.

Table III. Averaged energy absorption results for each rod configuration tested.

Type	Average Energy/Length (J/mm)	Average SEA (kJ/kg)	% Change	CV (%)
Baseline	0.15	59.8	-	4.50
Inline	0.20	77.7	30%	4.55
Parallel	0.32	62.4	4%	0.78

The additional work required by the loaded rod to compress the foam surrounding the next rod and then the work required to move that rod meant that energy absorption was generally higher for this configuration.

Compared to the values shown in Table II, the absolute energy absorbed during these tests was relatively small, roughly two orders of magnitude lower than the full sandwich coupons (approximately 1%). This value increases slightly when tufts rods are allowed to collide with each other, and increases significantly when parallel rods are loaded together. However, it should be noted that the tufted test coupons discussed previously featured approximately 30 tufts within them. As such, the overall contribution of the tuft drift mechanism can be considered to be a significant portion of the overall energy absorption of the structure. Results of this test suggests that for the tuft drifting mechanism to be of maximum benefit to the overall crushing performance then the tuft density within the sandwich panel should be high, to facilitate an increased number of tuft interactions. However testing has shown that collisions between tufts on a small scale can still add significant improvements to the energy absorption of a single tuft. If these collisions could be controlled, by forcing the path of the tuft during failure, a substantial increase to the energy absorbing efficiency of the structure could be made.

CONCLUSIONS

Experimental testing has been carried out to capture and evaluate the interior failure mechanism that occurs when tufted sandwich structures fail under edgewise crushing loads. Edgewise compression tests have been carried out and successfully demonstrated that tufts will drift through the foam core after failing locally, and this will lead to collisions and subsequent stacking of the tufts as crushing progresses. Follow up testing investigated the forces required to facilitate this behaviour, and thus the amount of energy absorbed. Results indicated that whilst on an individual level, the energy contribution of a single tuft is negligible, increased energy absorption is achieved when tufts are allowed to collide with each other. The results suggest that the cumulative effect of this behaviour over a larger panel with more tufts would mean that this mechanism does play a significant role within the energy absorption of a tufted sandwich structure, and thus could be incorporated into the design of future structures.

ACKNOWLEDGEMENTS

This work was supported by the Engineering and Physical Sciences Research Council through the EPSRC Centre for Doctoral Training in Advanced Composites for Innovation and Science (Grant: EP/G036772/1) and the EPSRC Centre for Innovative Manufacturing in Composites (CIMComp) (Grant: EP/IO33513/1).

REFERENCES

- [1] European Parliament and Council of the European Union. "Official Journal of the European Union" 2009;55.
- [2] Tucker N, Lindsey K. *An Introduction to Automotive Composites*. Rapra Technology Ltd; 2002.
- [3] Hara D, Özgen GO. "Investigation of Weight Reduction of Automotive Body Structures with the Use of Sandwich Materials." *Transp Res Procedia* 2016;14:1013–20.
- [4] Jacob GC, Fellers JF, Starbuck JM. "Energy Absorption in Polymer Composite Materials for Automotive Crashworthiness." *J Compos Mater* 2008;36:813–38.
- [5] Mamalis AG, Manolakos DE, Ioannidis MB, Papapostolou DP. "On the crushing response of composite sandwich panels subjected to edgewise compression: Experimental." *Compos Struct* 2005;71:246–57.
- [6] Nanayakkara AM, Feih S, Mouritz AP. "Improving the fracture resistance of sandwich composite T-joints by z-pinning." *Compos Struct* 2013;96:207–15.
- [7] Aktas A, Potluri P, Porat I. "Development of through-thickness reinforcement in advanced composites incorporating rigid cellular foams." *Appl Compos Mater* 2013;20:553–68.
- [8] Dell'Anno G, Treiber JW, Partridge IK. "Manufacturing of composite parts reinforced through-thickness by tufting." *Robot Comput Integr Manuf* 2016;37:262–72.
- [9] Tan G, Hartley J, Withers E, Kratz J. "Towards the Development of an Instrumented Test Bed for Tufting Visualisation." *SAMPE Eur. Conf.*, Amiens: 2015.
- [10] Dell'Anno G, Cartié DD, Partridge IK, Rezai A. "Exploring mechanical property balance in tufted carbon fabric/epoxy composites." *Compos Part A Appl Sci Manuf* 2007;38:2366–73.
- [11] Treiber JW. "Performance of tufted carbon fibre/epoxy composites." PhD Thesis, Cranfield University, 2011.
- [12] Osmiani C, Mohamed G, Treiber JW, Allegri G, Partridge IK. "Exploring the influence of micro-structure on the mechanical properties and crack bridging mechanisms of fibrous tufts." *Compos Part A Appl Sci Manuf* 2016;91:409–19.
- [13] Liu L, Zhang T, Wang P, Legrand X, Soulat D. "Influence of the tufting yarns on formability of tufted 3-Dimensional composite reinforcement." *Compos Part A Appl Sci Manuf* 2015;78:403–11.
- [14] Cartié DDR, Dell'Anno G, Poulin E, Partridge IK. "3D reinforcement of stiffener-to-skin T-joints by Z-pinning and tufting." *Eng Fract Mech* 2006;73:2532–40.
- [15] Deconinck P, Capelle J, Bouchart V, Chevrier P, Ravallier F. "Delamination propagation analysis in tufted carbon fibre-reinforced plastic composites subjected to high-velocity impact." *J Reinf Plast Compos* 2014;33:1353–63.
- [16] Henao A, Carrera M, Miravete A, Castejón L. "Mechanical performance of through-thickness tufted sandwich structures." *Compos Struct* 2010;92:2052–9.
- [17] Blok L, Kratz J, Lukaszewicz D, Hesse S, Ward C, Kassapoglou C. "Improvement of the in-plane crushing response of CFRP sandwich panels by through-thickness reinforcements." *Compos Struct* 2017;161:15–22.
- [18] Hartley JW, Kratz J, Ward C, Partridge IK. "Effect of tufting density and loop length on the crushing behaviour of tufted sandwich specimens." *Compos Part B Eng* 2017;112:49–56.
- [19] Elmarakbi A. *Advanced Composite Materials for Automotive Applications: Structural Integrity and Crashworthiness*. Chichester, UK: John Wiley & Sons Ltd; 2013.
- [20] Makabe C, Murdani A, Kuniyoshi K, Irei Y, Saimoto A. "Crack-growth arrest by redirecting crack growth by drilling stop holes and inserting pins into them." *Eng Fail Anal* 2009;16:475–83.